Tissue-specific and SRSF1-dependent splicing of fibronectin, a matrix protein that controls host cell invasion

Isabel Cristina Lopez-Mejia[a,b], Marion De Toledo[a], Flavio Della Seta[a], Patrick Fafet[a], Cosette Rebouissou[a], Virginie Deleuze[a], Jean Marie Blanchard[a], Christian Jorgensen[c,d], Jamal Tazi[a], and Marie-Luce Vignais[a,c]

[a]Institut de Génétique Moléculaire de Montpellier, CNRS UMR 5535/IFR122, Universities of Montpellier 1 and Montpellier 2, 34293 Montpellier Cedex 5, France; [b]Département de Physiologie, Université de Lausanne, CH-1015 Lausanne, Switzerland; [c]INSERM U844, Institut des Neurosciences de Montpellier, Centre Hospitalier Universitaire Saint Eloi, Université Montpellier 1, 34295 Montpellier Cedex 5, France; [d]Service Immuno-Rhumatologie, Centre Hospitalier Universitaire Lapeyronie, 34093 Montpellier Cedex, France

ABSTRACT Cell invasion targets specific tissues in physiological placental implantation and pathological metastasis, which raises questions about how this process is controlled. We compare dermis and endometrium capacities to support trophoblast invasion, using matching sets of human primary fibroblasts in a coculture assay with human placental explants. Substituting endometrium, the natural trophoblast target, with dermis dramatically reduces trophoblast interstitial invasion. Our data reveal that endometrium expresses a higher rate of the fibronectin (FN) extra type III domain A+ (EDA+) splicing isoform, which displays stronger matrix incorporation capacity. We demonstrate that the high FN content of the endometrium matrix, and not specifically the EDA domain, supports trophoblast invasion by showing that forced incorporation of plasma FN (EDA–) promotes efficient trophoblast invasion. We further show that the serine/arginine-rich protein serine/arginine-rich splicing factor 1 (SRSF1) is more highly expressed in endometrium and, using RNA interference, that it is involved in the higher EDA exon inclusion rate in endometrium. Our data therefore show a mechanism by which tissues can be distinguished, for their capacity to support invasion, by their different rates of EDA inclusion, linked to their SRSF1 protein levels. In the broader context of cancer pathology, the results suggest that SRSF1 might play a central role not only in the tumor cells, but also in the surrounding stroma.

INTRODUCTION

Cell invasion is a natural process required for the tissue-remodeling events that occur during physiological processes such as embryonic development and placental implantation. Failure to properly regulate cell invasion is responsible for life-threatening pathological conditions such as cancer metastases. Despite the abundance of data on the regulation of epithelial cell migration, essential questions remain partly unanswered. In particular, the set of cues received from the stromal microenvironment that determines epithelial cell migration properties and, in the case of cancer progression, metastasis migration endpoints, remains elusive. In other words, it is still unclear why some organs appear more prone than others to invasion by given epithelial cells, as has long been known for cancer metastases (Paget, 1889). Several hypotheses have been considered, involving both cellular and noncellular components of the microenvironment (Joyce and Pollard, 2009; Nguyen et al., 2009; Friedl and Alexander, 2011). Among the latter, the stroma-derived extracellular matrix (ECM), and more specifically the interstitial matrix, could be determinant in selectively providing the appropriate migration scaffold for given sets of epithelial cells (Lu et al., 2012).

Interactions between cells and their neighboring extracellular matrix network are highly dynamic and essential for the determination of cell behavior. The extracellular matrix consists of a heterogeneous network of fibrillar and nonfibrillar components whose assembly into functional structures appears highly regulated (Frantz et al., 2010). Collagens and fibronectin (FN) are major proteins of the connective tissue. Collagen fibrillogenesis occurs through complex interactions with noncollagenous molecules such as fibronectin, and the assembly of both collagen and fibronectin into fibrillar networks relies on interactions with cell surface integrin receptors (Mao and Schwarzbauer, 2005; Sottile et al., 2007; Kadler et al., 2008; Singh et al., 2010). Different collagen proteins, expressed from different genes, have been described, including the fibril-forming collagens I–III and V and the basement membrane collagen IV (Heino, 2007). In contrast, the various fibronectin isoforms found in the cellular environment result from the alternative splicing of a unique fibronectin-encoding gene at three sites: extra type III domain A (EDA)/EIIIA, EDB/EIIIB, and IIICS/V (White et al., 2008). The essential biological role played by FN and the EDA and EDB domains is supported by the embryonic lethality associated with both the FN knockout and the double deletion of the EDA and EDB exons (George et al., 1993; Astrof et al., 2007; White et al., 2008). The fibronectin EDA domain favors the formation of extensive fibrous networks that participate in the insoluble extracellular matrix. The EDA+ fibronectin is therefore referred to as cellular fibronectin (cFN; Manabe et al., 1997; Abe et al., 2005; Mao and Schwarzbauer, 2005; Zoppi et al., 2012). In contrast, the plasma FN (pFN) lacks both EDA and EDB exons and remains mostly soluble even though it can be incorporated, like cFN, into insoluble matrix (McKeown-Longo and Etzler, 1987; Peters et al., 1990; Moretti et al., 2007). The EDA containing fibronectin variant, also called fetal fibronectin for its expression during embryogenesis, is reexpressed in adult cells during tissue repair, tumor progression, and inflammation. The inclusion of the EDA domain depends on RNA secondary structure (Buratti and Baralle, 2004) and the recruitment and phosphorylation status of the Ser/Arg-rich (SR) protein serine/arginine-rich splicing factor 1 (SRSF1; alternative splicing factor/splicing factor 2; Mermoud et al., 1994; Cramer et al., 1997, 1999; Misteli et al., 1997, 1998; Kadener et al., 2002; Nogués et al., 2003; Blaustein et al., 2009; Chen and Manley, 2009; de la Mata et al., 2010; White et al., 2010) and is facilitated by a reduced pol II elongation rate (de la Mata et al., 2003, 2010; Munoz et al., 2010).

Placental implantation during pregnancy relies on the invasive capacity of trophoblast cells produced by the trophectoderm of the blastocyst. Trophoblast invasion of the maternal endometrium represents a natural invasion process that enables efficient placental implantation and subsequent nurturing of the developing embryo (Norwitz et al., 2001). Invasive trophoblast and cancer cells share striking similarities in their migration capacities and dependence on the surrounding stroma, albeit with the notable difference of an invasion process that remains controlled both in time and space in the case of placental implantation (Soundararajan and Rao, 2004). Of interest, in humans, the differentiation of the cytotrophoblast cells present in the placental villi into the invasive extravillous cytotrophoblast cells (EVCTs) is accompanied by an up-regulation of the expression of the laminin/collagen receptor α1β1 and fibronectin-binding integrin α5β1 (Damsky et al., 1994; Aplin et al., 1999; Harris et al., 2009).

To study the regulation of epithelial cell invasion, we previously developed a model system based on the invasion of the endometrial stroma by trophoblastic cells that occurs during human placental implantation (Fafet et al., 2008). This system is based on the coculture of human placental explants and primary endometrial fibroblasts. Because fibroblasts from different human anatomical sites display distinct transcriptional patterns (Chang et al., 2002; Rinn et al., 2006), we investigated whether the substitution of human endometrium fibroblasts with fibroblasts from an unrelated close-by human organ could affect trophoblast invasion properties. Using matching sets of tissue samples from patients, we found that dermis is much less efficient than endometrium in supporting trophoblast interstitial migration, a phenomenon related to the fibronectin content of the extracellular matrix of these tissues. Fibroblasts from human endometrium expressed more of the EDA+ fibronectin-splicing isoform, resulting in denser fibronectin meshworks and a higher capacity to support efficient trophoblast invasion. Of note, we found that the higher expression rate of the fibronectin EDA+ splicing isoform in endometrium results from higher expression levels of the SR protein SRSF1 in fibroblasts from this tissue. These data show how, through alternative splicing, the cellular concentrations of the splicing factor SRSF1 can give unique properties to tissues and enable host cell invasion.

RESULTS

Endometrial and dermal fibroblasts exhibit distinct capacities in fostering trophoblast interstitial migration

We previously set up an ex vivo model system mimicking human placental implantation (Fafet et al., 2008). It is based on the coculture of primary endometrial fibroblasts and explants from 4- to 7-wk placentas. To investigate the role of the stromal cell matrix for EVCT migration, we tested the effect of the substitution of endometrium with the unrelated, but close-by, subpubic dermis tissue. For that purpose, we isolated matching sets of primary human fibroblasts from dermis and endometrium specimens obtained from four different patients undergoing C-sections. Cocultures were set up between placental villi and fibroblasts isolated either from endometrium (the biologically relevant tissue) or dermis. Trophoblast migration was then followed by phase-contrast time-lapse microscopy (Figure 1A and Supplemental Videos S1 and S2). As we previously observed (Fafet et al., 2008), trophoblast explants attached to the endometrial fibroblast layer and within 24 h produced EVCTs that demonstrated the capacity to individually migrate within the endometrial fibroblast layer, away from the trophoblast explants that remained immobile (Figure 1A, left). On dermis, however, we unexpectedly observed further movement of the attached trophoblast villi (see left villus movement indicated by arrowheads). Most of all, EVCTs displayed a superficial migration on the dermis fibroblast layer instead of the interstitial EVCT migration observed with endometrial fibroblasts (Figure 1A, right). Time-lapse experiments, with pictures taken every 8 min for 24–48 h, were decisive in understanding this phenomenon of superficial migration of EVCTs that were characterized by high refringency and could eventually detach from the underlying dermis fibroblast layer. Phase-contrast time-lapse microscopy was performed on trophoblastic villi from two other placentas and led to similar observations (data not shown). To confirm and quantify these trophoblast migration differences, we tested three additional placentas and three different sets of fibroblasts (from both endometrium and dermis). Phase-contrast images of the cocultures were taken 24 h apart, and both villi movement and trophoblast superficial migration between these two time points were scored (Figure 1B). As observed in the time-lapse experiments, villi movements occurred more frequently on dermis (37% of the villi) than on endometrium (15%). Similarly, EVCT superficial migration occurred for 60% of the villi
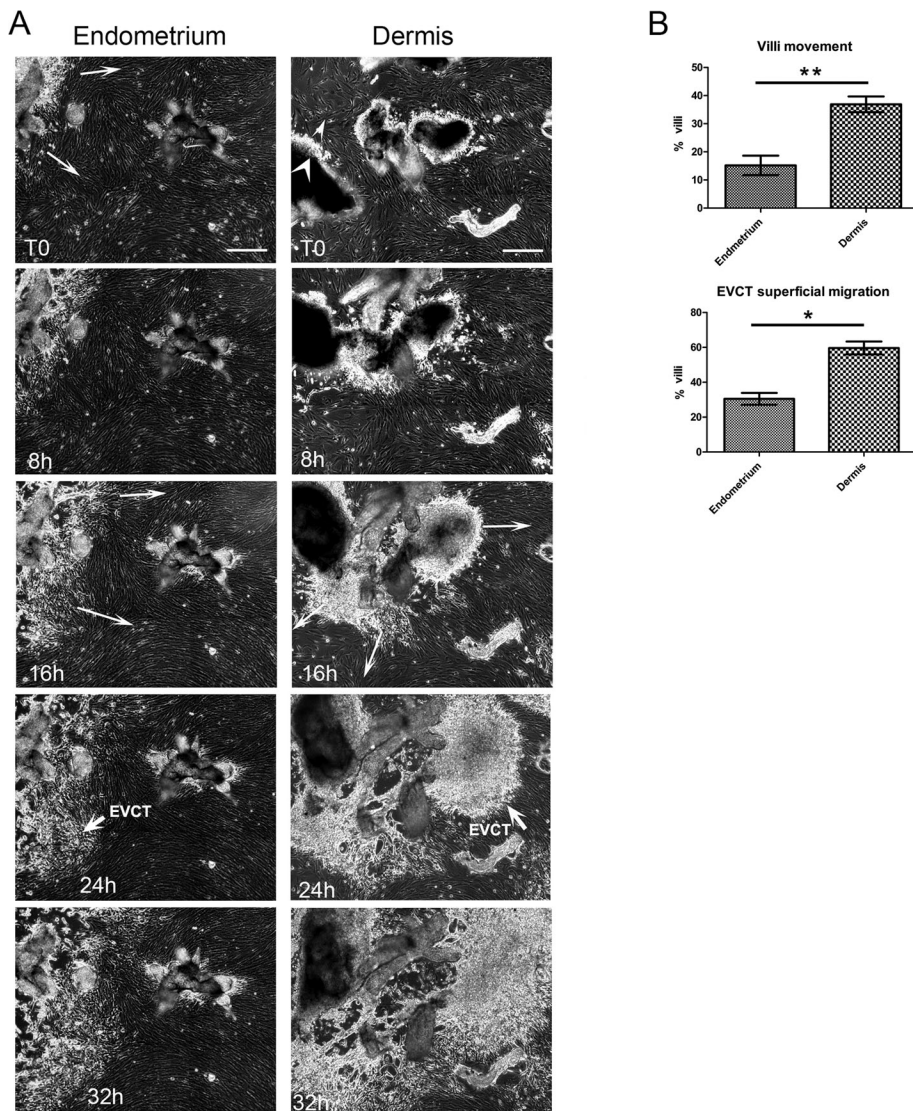
A Endometrium   Dermis

B

Villi movement

EVCT superficial migration

FIGURE 1: Endometrium and dermis fibroblasts show distinct capacities in fostering EVCT migration. Human placental explants were seeded on confluent layers of endometrium or dermis human primary fibroblasts. Sixteen hours later, the culture plates were rinsed several times to discard all unbound villi. (A) Migration of EVCTs produced by the trophoblast villi was followed by phase-contrast time-lapse microscopy of camera-scanned fields (nine contiguous fields). T0 is the beginning of the time lapse. Left, EVCTs exiting from the trophoblast villi and migrating with the endometrium cell layer (EVCT migration movements indicated by arrows; see Supplemental Video S1). On dermis (right), movement of the villi explants were observed (arrowheads), and EVCT cells appeared much more refringent and performed a superficial migration instead of the interstitial migration observed on endometrium (Supplemental Video S2). Bar, 300 μm. Similar findings were obtained with two other placentas. (B) Statistical analysis of trophoblastic villi mobility and EVCT superficial migration for cocultures with either endometrium or dermis fibroblasts. Data were obtained with trophoblastic villi (290 analyzed on endometrium and 240 on dermis) isolated from three placentas (in addition to the three placentas used in the time-lapse experiments) and three matching sets of fibroblasts, altogether used in five different combinations. Phase-contrast images of the cocultures were taken 24 h after seeding the trophoblastic explants and again 24 h later. Villi movement and EVCT superficial migration between these two time points were evaluated. Mean values with SEM. Two-tailed p values were determined with the Mann–Whitney rank sum test; **$p = 0.008$; *$p = 0.01$.

on dermis in comparison to only 30% on endometrium. Taken together, these findings indicate that endometrium and dermis fibroblasts display different capacities in supporting EVCT interstitial migration.

EVCTs exhibit different cytoskeleton structures and integrin expression patterns depending on whether they migrate on endometrium or dermis fibroblasts

We next asked whether the differences in EVCT migration patterns on dermis and endometrium were linked to differences in EVCT cytoskeleton and adhesion protein expression patterns. To address this, we performed confocal immunofluorescence microscopy of the cocultures (Figure 2). Striking differences were found in the trophoblast F-actin networks. EVCTs migrating on dermis fibroblasts could readily be identified by their well-defined actin bundles, a feature that was not observed on endometrium for EVCTs, otherwise identified by cytokeratin 7 expression (Figure 2A). The trophoblast integrin repertoire shifts from α6β4 within the villi to α1β1 and α5β1 during EVCT migration (Harris *et al.*, 2009). Consistent with this, we detected EVCT expression of both integrins α5 and α1 in the cocultures. Of interest, integrin α5 and α1 staining also underlined the formation of multiple cellular protrusions for EVCTs migrating on dermis compared with EVCTs migrating on endometrium (Figure 2, B and C). These data confirm the differences in EVCT migration characteristics depending on the type of fibroblasts—dermis or endometrium—that support their migration.

Dermis and endometrium fibroblasts express different ECM components

To understand the molecular bases for the different capacities of endometrium and dermis fibroblasts to support EVCT interstitial migration, we further characterized these fibroblasts for their expression of adhesion molecules and ECM components. Phase-contrast microscopy showed that dermis fibroblasts exhibited a distinct cell morphology, with a smoother membrane outline than endometrial fibroblasts (Figure 3). The adhesion pattern of the two types of fibroblasts also differed, as shown by the expression pattern of vinculin and integrin αV, an integrin highly expressed by both types of fibroblasts. Instead of the staining observed throughout the cell surface for endometrial fibroblasts, these proteins were found clustered into elongated peripheral structures in dermis fibroblasts (Figure 3). These differences prompted us to determine, by reverse transcription-quantitative PCR (RT-qPCR), the expression levels of ECM and adhesion proteins in both types of fibroblasts. Four sets of dermis and endometrium fibroblasts from four different donors were used. The expression levels of adhesion proteins and of most of the ECM components were found to be similar in
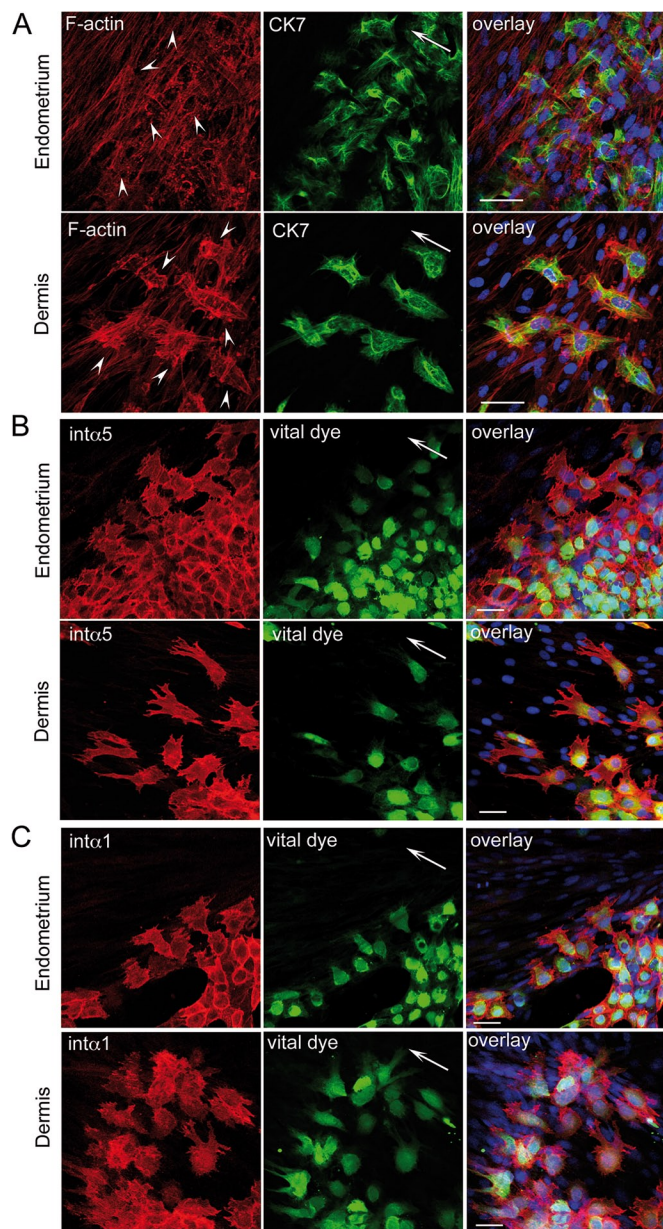
FIGURE 2: Cytotrophoblast cells display different actin cytoskeleton structures, depending on the supporting fibroblast matrix. Placental explants were cocultured with either endometrium or dermis fibroblasts for 40 h, at which point cells were fixed and stained for F-actin, cytokeratin 7, and integrins α5 and α1. (A) F-actin labeling of the cocultures shows a strong cortical staining for EVCTs, identified by cytokeratin 7 expression, when they migrate on the dermis fibroblast layer. (B, C) Integrin α5 (intα5) and α1 (intα1) labeling. Trophoblast explants were labeled with a green vital dye before the coculture with fibroblasts. After the coculture, cells were fixed and stained with the integrin antibodies. Similar results were observed in three independent experiments, with villi isolated from different placentas and tested on matching sets of dermis and endometrium fibroblasts isolated from different donors. Nuclear staining with Hoechst is shown in the overlays. Confocal microscopy sections. Arrows indicate the direction of EVCT migration. Arrowheads indicate EVCT positions. Bar, 50 μm.

FIGURE 3: Endometrium and dermis fibroblasts display different characteristics, as exemplified by the vinculin and integrin αV expression patterns. The primary human fibroblasts isolated from endometrium and dermis tissues were compared for their cell morphology, as shown by phase-contrast microscopy, as well as for their actin network organization, visualized by rhodamine–phalloidin, and vinculin and integrin αV staining. Four matching sets of endometrial and dermal fibroblasts were tested and yielded similar images. Confocal microscopy sections are shown with nuclei stained with Hoechst. Bar, 50 μm; higher magnification, 10 μm.

endometrial and dermal fibroblasts (Figure 4). Striking differences were observed for fibronectin, however, with a 2.5-fold-higher expression level in de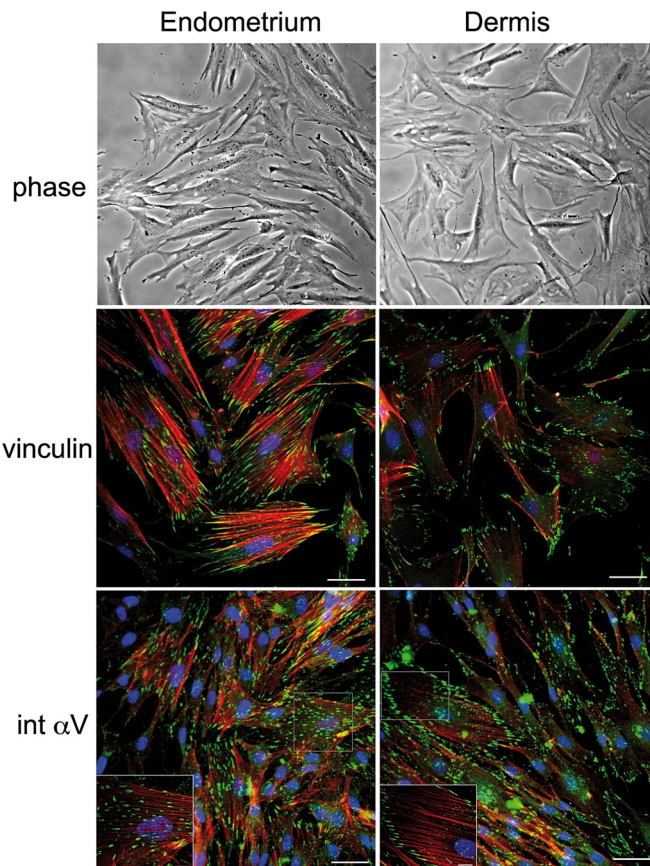rmis, and for collagen IV, present at low levels in endometrium but barely detectable in dermis. Collectively these data show that human endometrium and dermis fibroblasts express mostly similar levels of adhesion proteins and ECM components, with the notable exceptions of fibronectin and collagen IV. We further focused on fibronectin. To confirm biochemically the RT-qPCR data, we tested cell extracts obtained by direct Laemmli buffer lysis of the cell cultures, which therefore contain both cellular and ECM proteins (Figure 4B, bottom, ECM+C). Quite unexpectedly, with regard to the RT-qPCR data, the protein fraction corresponding to the ECM and intracellular content of endometrium fibroblasts showed a higher fibronectin content than for dermis. Because the secreted fibronectin can remain as a soluble protein in the culture medium, we also analyzed the fibronectin content of this protein fraction (Figure 4B, top, fibroblast culture supernatant). We found that dermis fibroblasts release much more soluble fibronectin in the culture medium than endometrium fibroblasts. This high fibronectin protein concentration in the dermis culture medium was in agreement with the high fibronectin expression rate detected in dermis fibroblasts at the RNA level. Of importance, it also suggested that fibronectin produced by endometrium and dermis fibroblasts have different properties.
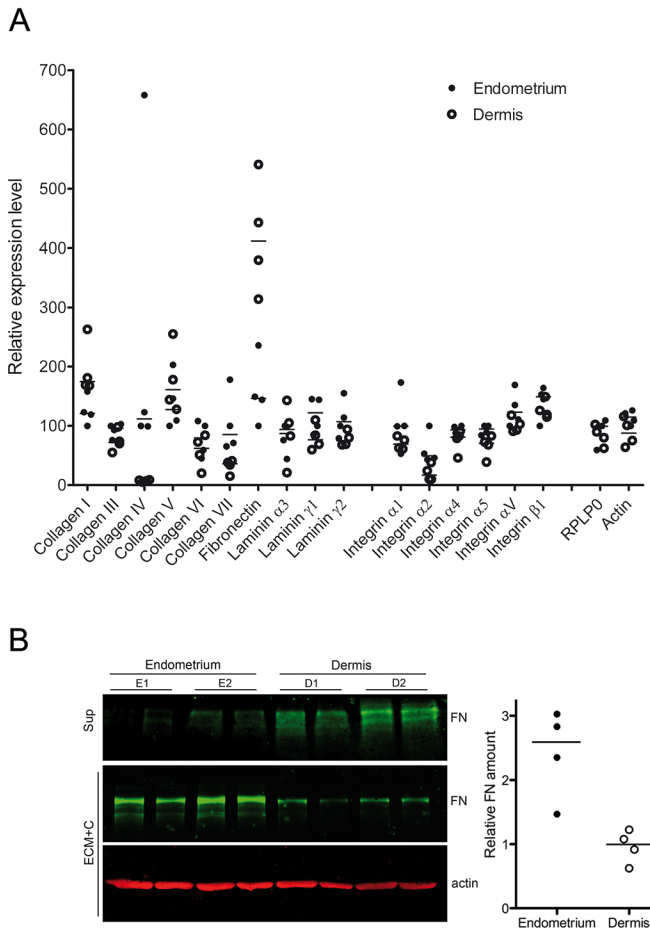
FIGURE 4: Expression of ECM components and adhesion molecules by endometrium and dermis fibroblasts. (A) RNAs were prepared from two independent cultures for each of four matching sets of dermis and endometrium fibroblasts. The relative expression levels of extracellular matrix components and adhesion molecules were determined by RT-qPCR. Data obtained for each endometrium (●) and dermis (○) primary cell line are plotted, and the corresponding median bars are indicated. The ribosomal phosphoprotein RPLP0 and actin were used as controls. (B) Protein fractions corresponding to the culture supernatants (Sup) and the ECM and cellular proteins (ECM + C) from matching sets of endometrium (E) and dermis (D) fibroblasts were analyzed by Western blot (left). The fibronectin (FN) and actin amount in the ECM+C fraction was quantified with the Odyssey system (LI-COR, Lincoln, NE). The fibronectin amounts relative to actin are plotted with an indication of the median value for both the endometrium (●) and dermis (○) cultures (right).

Endometrium and dermis fibroblasts express different fibronectin-splicing isoforms that influence the ECM fibronectin network

The distinct localization patterns for the fibronectin expressed by the endometrium and dermis fibroblasts, added to the known alternative splicing regulation of fibronectin, prompted us to further investigate which FN isoforms were expressed in these cells. RT-PCRs were performed on endometrium and dermis fibroblasts with sets of primers encompassing the alternatively spliced EDA, EDB, and IIICS, respectively (Supplemental Table S1). Analysis of the fibronectin PCR products by gel electrophoresis showed that endometrium and dermis fibroblasts express different fibronectin-splicing

isoforms, whose nature was confirmed by the PCR product sequencing (Figure 5A). To quantify the exon inclusion efficacy, we amplified the three FN regions by endpoint RT-PCR and measured the size and abundance of each amplicon by capillary electrophoresis using Caliper reading stations. For each of the fibronectin alternatively spliced regions, the relative abundance of the splicing isoforms was determined as a "percent spliced-in" (PSI) value, that is, the ratio of concentration of the long amplicon over the sum of those of the short and long amplicons (Venables et al., 2013). The level of EDA exon incorporation in endometrial fibroblasts was important and double the level found in dermis fibroblasts, as measured on RNAs isolated from matching sets of fibroblasts from four different donors (Figure 5A, right). In contrast, the inclusion rate of the EDB exon was low in both endometrium and dermis fibroblasts. There, too, the alternative exon inclusion level in dermis fibroblasts was half the level found in endometrium fibroblasts. In addition, no difference was observed in the splicing profiles of the IIICS alternatively spliced region between the two types of fibroblasts. Because of the overall low rate of EDB exon inclusion in both endometrial and dermis fibroblasts, we further focused on the EDA exon inclusion. Other splicing events, besides fibronectin, were compared between endometrium and dermis fibroblasts. Of interest, the inclusion of the FN EDA exon in endometrium fibroblasts was near the top of the list of events whose splicing varied between endometrium and dermis fibroblasts, only second in the series of 46 tested alternatively spliced events (Supplemental Table S2) to the use of a 3' splice site in p53-induced death domain protein (LRDD) pre-mRNA. Remarkably, alternative splicing for LRDD and apoptotic peptidase–activating factor 1 (APAF1), the two other genes whose splicing pattern greatly differs between dermis and endometrium fibroblasts, showed a reverse regulation and was instead favored in dermis fibroblasts. Because the EDA+ fibronectin isoform was reported to demonstrate higher ECM recruitment capacities than the EDA– isoform (Manabe et al., 1997; Abe et al., 2005; Mao and Schwarzbauer, 2005; Zoppi et al., 2012), we further tested biochemically the amount of ECM-bound FN for both types of fibroblasts by performing a deoxycholate extraction of the insoluble matrix (Pankov and Yamada, 2004). We found indeed that the ECM isolated from endometrium fibroblasts contained more fibronectin—both total FN and EDA+ FN—than the dermis ECM (Figure 5B). We tested whether we could supplement the dermis culture with commercially available plasma fibronectin (EDA– FN) so as to increase the FN concentration in the ECM, as suggested by previous work (McKeown-Longo and Etzler, 1987; Peters et al., 1990; Moretti et al., 2007). Addition of increasing amounts of plasma fibronectin (5–50 μg) to the culture resulted in more fibronectin in the culture medium, as expected (Figure 5C, top). As previously described (McKeown-Longo and Etzler, 1987; Peters et al., 1990; Moretti et al., 2007), addition of EDA– FN for 8 h to the dermis fibroblast culture also resulted in more FN in the protein fraction containing the ECM and cell content. This increase in fibronectin was found to be EDA– and therefore due, indeed, to the added plasma fibronectin (Figure 5C, bottom and quantification). Using the settings of the coculture, we supplemented the dermis culture with exogenous plasma fibronectin (50 μg of pFN [EDA–]/35-mm dish) 3 d before the protein extraction. We found that, in these conditions, the ECM concentrations of FN in the FN-supplemented dermis culture increased to levels close to those found in the endometrium cultures (Figure 5B). We also observed a slight increase in EDA+ FN in the supplemented dermis ECM. Because short-term plasma FN supplementation did not show this effect, we presume it might be explained by an increased recruitment of the EDA+ FN produced by the dermis fibroblasts over the 3-d period, by
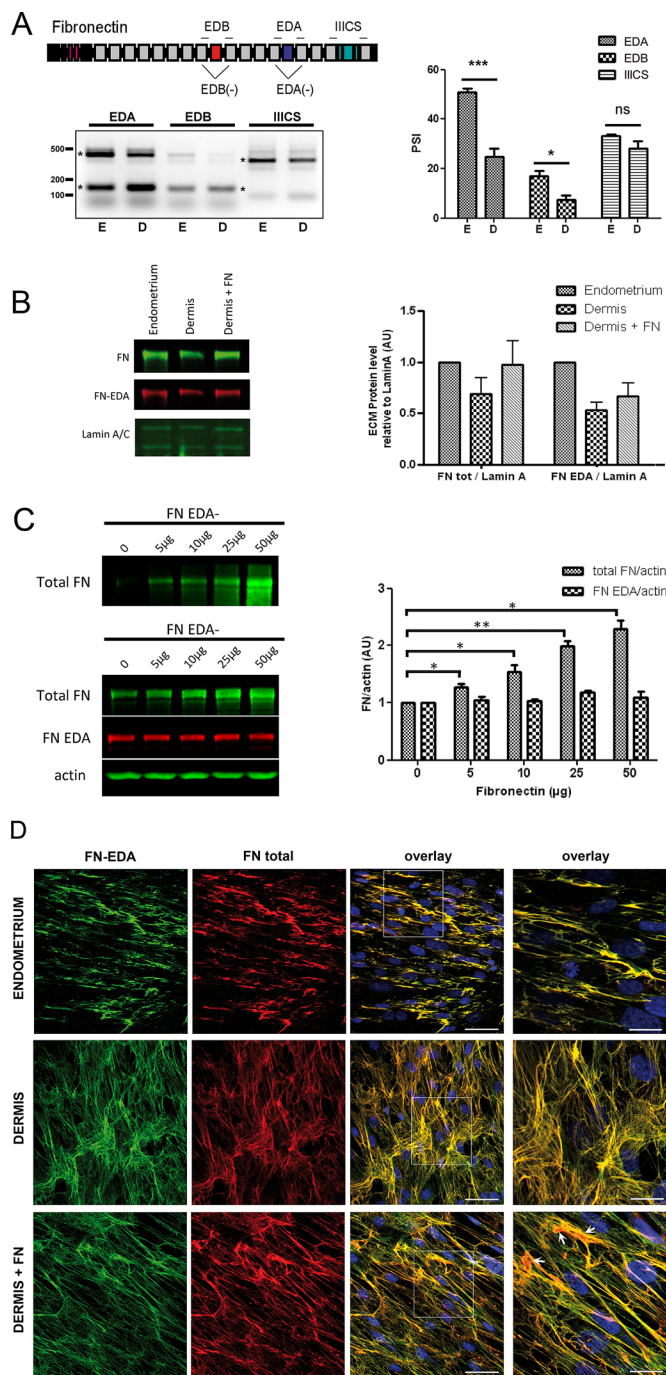
FIGURE 5: Endometrium and dermis fibroblasts express different fibronectin-splicing isoforms, leading to different matrix patterns. (A) Fibronectin alternative splicing in endometrium and dermis fibroblasts was tested by RT-PCR using primers encompassing the alternatively spliced EDA, EDB, and IIICS regions, respectively. The PCR products were analyzed by gel electrophoresis (DNA size markers in base pairs). The inclusion/exclusion of the exons was further confirmed by sequencing of the DNA from the bands marked with asterisks. Right, PSI values determined for the three FN exons, EDA, EDB, and IIICS, for endometrium (E) and dermis (D) fibroblasts obtained from four different donors. (B) Protein samples corresponding to the insoluble matrix fractions (deoxycholate extraction) from matching sets of endometrium and dermis fibroblasts, as well as of the dermis fibroblasts supplemented with plasma fibronectin for 3 d (+FN), were analyzed by Western blot, using an intermediate filament, lamin A/C, as a loading control. The

the law of mass action. We also analyzed, by immunofluorescence staining, the pattern of the ECM fibronectin generated by endometrium and dermis fibroblasts. Of interest, endometrium fibroblast cultures produced thick fibronectin bundles, in comparison to the fine, fibrillar FN matrix produced by dermis fibroblasts (Figure 5D). Double immunofluorescence staining of total and EDA+ fibronectin showed that the addition of plasma FN to the dermis fibroblast culture indeed led to the incorporation of EDA– FN into the ECM. Moreover, in several instances, the fine dermis FN structure was modified to form endometrium-like FN bundles upon EDA– FN supplementation. Taken together, our data show that 1) endometrium and dermis fibroblasts express different fibronectin splicing isoforms, with a higher EDA exon incorporation rate in endometrium compared with dermis; 2) even though endometrial fibroblasts express less total fibronectin than dermis, the fibronectin they produce generates an extracellular matrix that contains more fibronectin and is structured in thicker fibrils than dermis; and 3) addition of exogenous plasma fibronectin (EDA–) to the dermis fibroblast cultures increases their ECM FN content.

Fibronectin-enriched ECM enhances EVCT invasion

To assess the role of fibronectin in the differences observed between dermis and endometrium for trophoblast interstitial invasion, we supplemented the dermis fibroblasts with fibronectin and tested the effects on EVCT migration. Dermis fibroblasts were plated in the presence or absence of plasma fibronectin, along with endometrium fibroblasts. Three days later, the cocultures were set up as previously described, and two sets of phase-contrast pictures were taken 24 h apart for each of the three conditions: endometrium, dermis, and dermis supplemented with fibronectin (Figure 6A). Data obtained with endometrium and dermis fibroblasts confirmed our previous observations (Figure 6B; also see Figure 1). Moreover, addition of fibronectin to the dermis cell layer significantly modified trophoblast migration properties (Figure 6B). It lowered the occurrence of moving villi from 36 to 15% ($p = 0.036$). Most of all, it decreased the rate of EVCT superficial mass migration from 59 to 37% ($p = 0.015$), thus providing EVCT migration properties close to those observed with the endometrial cell matrix.

To dismiss other contributions from fibroblasts in the effects we observed, we used an artificial system—a synthetic three-dimensional (3D) collagen I matrix supplemented or not with plasma fibronectin—to test the effect of fibronectin on trophoblast

total and EDA-containing fibronectin amounts were quantified with the Odyssey system. The fibronectin amounts relative to lamin A are plotted. (C) Increasing amounts of plasma fibronectin were added to dermis cultures for 8 h. The protein fraction corresponding to the culture supernatant (top) and the ECM and cell content (bottom) were analyzed for their content in total FN and in EDA+ FN. The amounts of FN protein were quantified and are shown in the graph. For total FN: 5 µg, $p = 0.0481$ (*); 10 µg, $p = 0.0440$ (*); 25 µg, $p = 0.00891$ (**); 50 µg, $p = 0.0120$ (*). No significant differences were found for the content in EDA+ FN, with p ranging from 0.6025 to 0.9237. (D) Endometrium and dermis fibroblasts were seeded in the same conditions as for the cocultures. For the fibronectin supplementation conditions (dermis+ FN), pFN was added to dermis fibroblasts at the time of the culture. Four days later, cultures were fixed and stained for total fibronectin (FN total), EDA-containing fibronectin (FN– EDA), and Hoechst (shown in the overlays). Confocal microscopy sections. Bar, 100 µm; higher magnification, 20 µm. Arrows show FN that is presumably EDA–, as it was bound by the anti-FN antibody (stained in red) and not by the anti–FN EDA antibody.

A

T0 | T24

ENDOMETRIUM

DERMIS

DERMIS + FN

B

Villi movement

% moving villi

Endometrium | Dermis | Dermis +Fn

** | *

EVCT superficial migration

% mass migration
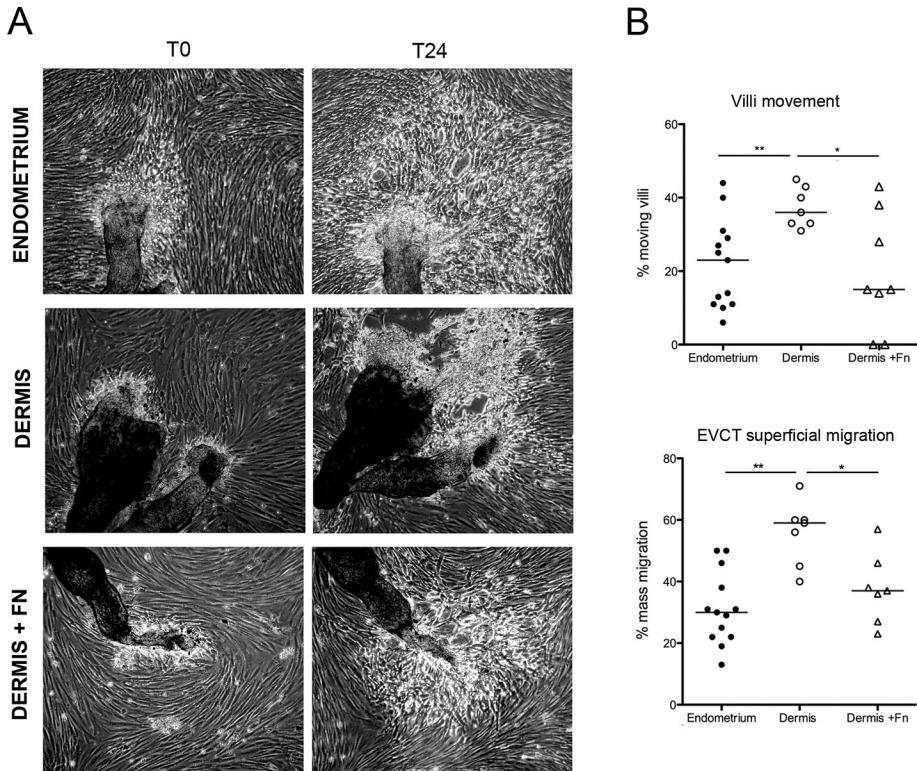
Endometrium | Dermis | Dermis +Fn

** | *

FIGURE 6: Fibronectin supplementation of the dermis cell layer enhances trophoblast interstitial migration. Cocultures were set up between human trophoblast explants and endometrial fibroblasts, dermal fibroblasts, or dermal fibroblasts supplemented with plasma fibronectin. After 16 h of coculture, phase-contrast pictures were taken (T0) and again 24 h later (T24h). (A) Phase-contrast micrographs show interstitial EVCT migration for cocultures on endometrium and fibronectin-supplemented dermis fibroblasts and superficial EVCT mass migration (refringent packed EVCTs) in dermis coculture conditions. (B) The type of EVCT migration (superficial vs. interstitial), as well as the occurrence of trophoblast villi movement, were analyzed in the three coculture conditions. Data points corresponding to each of the independent cultures are plotted, and the median values are indicated. Two-tailed p values were determined with the Mann–Whitney rank sum test. For villi movement, $**p = 0.007$, $*p = 0.036$; for EVCT migration, $**p = 0.002$, $*p = 0.015$.

domain but instead a high fibronectin concentration within the matrix that is essential for migration.

The high expression level of SRSF1 in endometrium contributes to FN EDA exon inclusion

To determine the reason for the higher incorporation rate of the EDA exon in endometrium fibroblasts, we focused on SR proteins, a family of proteins involved in the regulation of alternative splicing. Because their activity depends on their phosphorylation status, we first compared the phosphorylation patterns of SR proteins in endometrium and dermis fibroblasts using the mAb104 antibody, which recognizes a phosphoserine epitope in the RS domain of SR proteins (Zahler et al., 1993). We observed a stronger signal in the endometrial cell lines tested than in their matching dermal counterparts (Figure 8A). This difference was specific to SR proteins because the phosphorylation levels of the extracellular signal-regulated protein kinase ERK, tested in the same protein extracts, showed no difference. We further focused on the SR protein SRSF1, which has extensively been shown to favor the inclusion of the fibronectin EDA domain (Mermoud et al., 1994; Cramer et al., 1997, 1999; Misteli et al., 1997, 1998; Kadener et al., 2002; Nogués et al., 2003; Blaustein et al., 2009; Chen and Manley, 2009; de la Mata et al., 2010; White et al., 2010). Preparing cell extracts from endometrium and dermis fibroblasts, we found a twofold higher SRSF1 protein expression level in endometrium than in dermis (Figure 8B). Because the localization and in vivo activity of SR proteins depend on their phosphorylation status, we investigated SRSF1 phosphorylation by two-dimensional (2D) gel electrophoresis. Indeed, previous studies on various cell lines in our laboratory showed that SRSF1 can be distributed in at least 10 different spots in 2D gels, corresponding to different phosphorylation isoforms. Most of the phosphorylation sites are in the RS domain containing the SR repeats. Comparing extracts from endometrium and dermis fibroblasts, we observed similar spots, at the same migration distance, for endometrial and dermal extracts, which implied the same extent of phosphorylation of SRSF1 (Figure 8C). The stronger SRSF1 signal in the endometrium extracts was also in agreement with the twofold-higher SRSF1 protein concentration found in endometrium compared with dermis (Figure 8B).

To determine whether the higher expression levels of SRSF1 observed in endometrial fibroblasts were responsible for the increased EDA exon incorporation, we tested the effect of SRSF1 silencing in these cells. RNA interference–mediated depletion of SRSF1 led indeed to a twofold reduction of the EDA+ fibronectin protein concentration while having no effect on the total fibronectin concentration (Figure 9A). This reduced inclusion of the EDA alternative exon in response to SRSF1 silencing was also observed at the RNA level (Figure 9, B and C). The effects of SRSF1 depletion on exon inclusion were performed and quantified by capillary electrophoresis
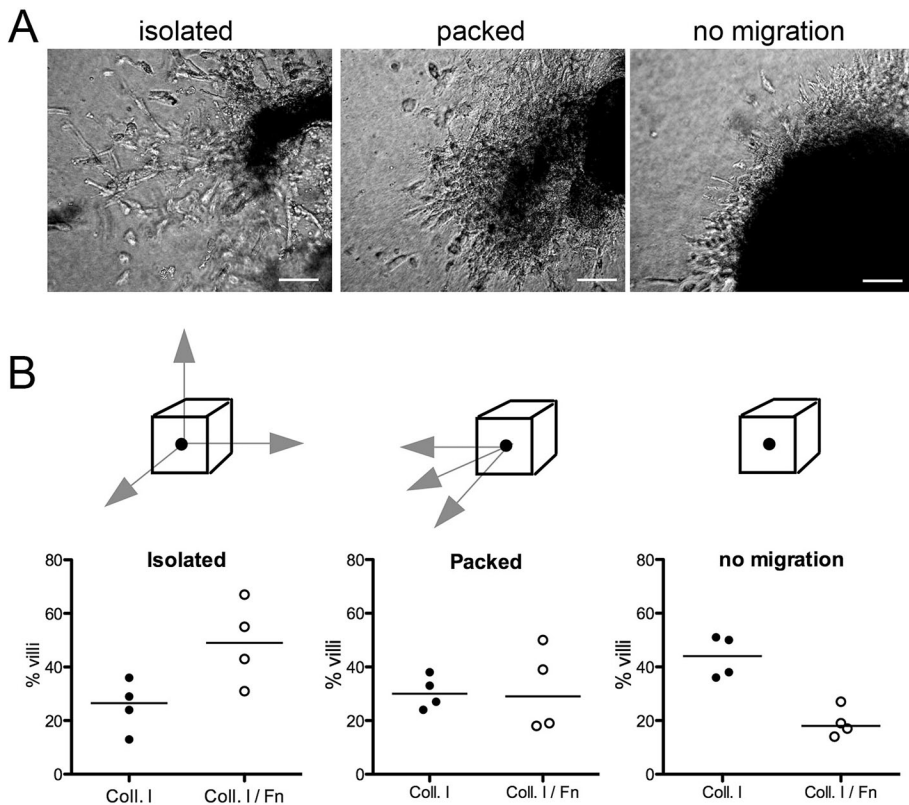
migration. Placental explants were embedded in the matrix and, within 24–48 h, released EVCTs that could migrate away from the explants. On the basis of phase-contrast images of the cultures taken at day 4, EVCT migration phenotypes were classified into three categories: "isolated" migration achieved by EVCTs that migrated as single cells in all directions, "packed" EVCT migration occurring mainly in a single direction with few isolated cells, and "no migration" for EVCTs demonstrating a low capacity to migrate away from the trophoblast villi (Figure 7A). The statistical analysis was performed on EVCTs produced by villi dissected from four different placentas. Whereas isolated EVCT 3D migration was achieved for only 25% of villi in the collagen I matrix, supplementation of the matrix with fibronectin raised this proportion to roughly 50% (Figure 7B). Conversely, the percentage of villi displaying a low migration phenotype decreased twofold on addition of fibronectin. The percentage of villi producing EVCTs of the "packed" phenotype remained unchanged on addition of fibronectin. These data show that addition of fibronectin within the matrix enhances isolated EVCT 3D migration, that is, EVCT invasion capacity. Together these data, in addition to those obtained in the coculture settings, support a role for fibronectin in providing an adequate matrix for interstitial EVCT migration. Of importance, the fact that plasma fibronectin (EDA–) can enhance migration indicates that it is not the presence of the EDA

FIGURE 7: Fibronectin supplementation of a synthetic 3D collagen I matrix promotes isolated trophoblast cell migration. Trophoblastic villi were embedded within a 3D collagen I matrix (coll I) supplemented with plasma fibronectin when indicated (coll I/Fn). At day 4, phase-contrast pictures of the cultures were taken. Three types of EVCT migration were identified for coll I/Fn cultures (A; schematized in B): "isolated" migration, corresponding to the migration of single EVCTs in all directions; "packed" cell migration; and "no migration," for EVCTs showing a low capacity to migrate away from the trophoblastic villi. Bar, 100 µm. (B) Statistical analysis of EVCT migration in coll I and coll I/Fn 3D culture conditions. Data were obtained with villi isolated from four placentas (>100 trophoblastic villi analyzed in each condition). For each placenta, the number of villi giving rise to each type of EVCT migration was rated and is expressed as a percentage of the total number of villi for this placenta. The median value is indicated for 3D cultures performed in collagen I (●) or in collagen I supplemented with plasma fibronectin (○).

higher EDA exon incorporation rate in endometrium.

DISCUSSION

The stromal microenvironment influences epithelial cell migration. We tested here whether fibroblasts from different tissues display similar capacities to support migration. Instead of the interstitial trophoblast migration previously observed on endometrium (Fafet et al., 2008), we observed superficial EVCT migration on dermis. We found that fibronectin is differently provided by endometrium and dermis and greatly responsible for these differences. Moreover, the higher EDA inclusion rate in endometrium fibronectin can be explained, at least in part, by the higher concentrations of the splicing factor SRSF1. Our data thus establish a relationship between the capacity of a tissue to support invasion, the regulation of alternative splicing, and the expression level of splicing factors.

We showed that addition of plasma FN (EDA–) enhanced the invasive capacity of EVCTs, in both the fibroblast coculture system and a 3D collagen I matrix. These data suggest that the documented trophoblast-secreted fibronectin (Feinberg et al., 1991; Bischof et al., 1995; Aplin et al., 1999) is not sufficient to modify the ECM structure and ensure its own migration. Additional contributions from the stroma-derived matrix are required. They also show that EVCT interstitial migration requires high fibronectin concentrations but not the EDA exon, as supplementation of the culture with plasma fibronectin (deprived of the EDA domain) can recapitulate matrix properties of the endometrium fibroblasts. This raises the question of why dermis fibroblasts, which express high concentrations of EDA– fibronectin, cannot provide an ECM proper to support trophoblast interstitial migration. Our hypothesis for this apparent discrepancy is that, although EDA– FN demonstrates a capacity to incorporate within the insoluble ECM, as previously demonstrated (Moretti et al., 2007) and confirmed here, this fibrillogenesis capacity is much poorer than that of the EDA+ FN (Guan et al., 1990; Abe et al., 2005). This explains why dermis-derived fibronectin is observed in high amounts in the culture supernatant but in low amounts in the insoluble matrix. It can also explain to some extent why, despite their higher fibronectin RNA expression levels, dermis fibroblasts generate a fibronectin matrix less prone than that of endometrium to promote EVCT invasion. Other factors may contribute to the differences observed between endometrium and dermis FN networks. Because FN interacts with other matrix components, such as collagens, in the process of fibrillogenesis (Kadler et al., 2008), the different expression levels of collagen IV in endometrium and dermis might also contribute to the distinct FN networks observed and, in a more general manner, to different matrix structures for endometrium and dermis. FN assembly is a cell-mediated process that depends on the cytoskeleton traction forces, and therefore the dynamic interactions between FN and the actin cytoskeleton at the
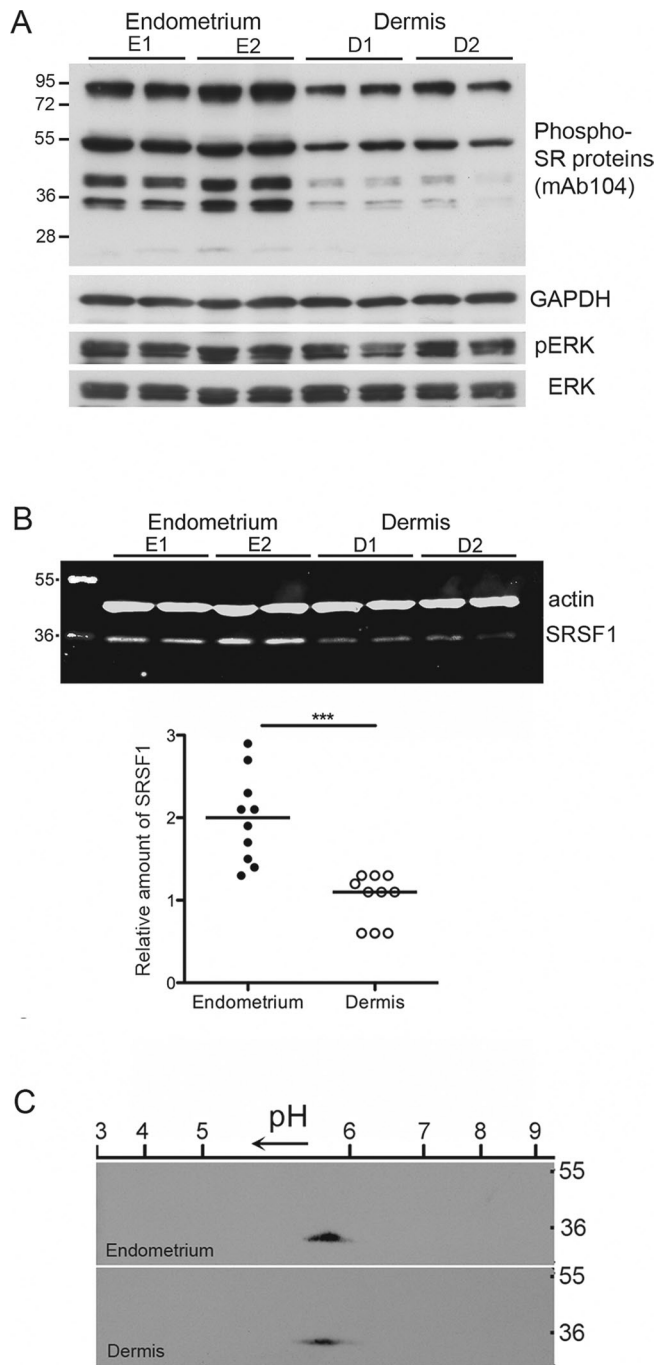
at the high-throughput PCR platform of Sherbrooke University (Sherbrooke, Canada). Despite higher overall PSI values than ours, presumably due to different reaction conditions and primer sequences (Supplemental Table S3), similar differences in the EDA inclusion rate between endometrium and dermis were observed. Of importance, SRSF1 depletion showed a twofold decrease of the FN EDA PSI value, whereas the inclusion of the EDB exon remained unchanged (Figure 9, B and C). The EDA exon skipping induced by the SRSF1 knockdown represented the third-most-changed alternative splicing event among the 46 splicing events tested, just after the alternative splicings of LRDD and APAF1. It is worth noting that insulin receptor (INSR) was also in the top list of genes whose exon inclusion was affected by SRSF1 depletion, as the inclusion of INSR exon 11, like that of FN EDA, is enhanced by SRSF1 (Sen et al., 2009). These data show that inclusion of the FN EDA exon in endometrium fibroblasts is linked to the expression levels of the SR protein SRSF1. Overall our data show that the higher capacity of endometrium fibroblasts to support interstitial EVCT migration is due to their capacity to produce a matrix enriched in fibronectin, which is linked to the expression of the EDA-containing fibronectin isoform (Figure 10). We provide a mechanism by which the higher SRSF1 cellular concentrations in endometrial fibroblasts contribute to this

FIGURE 8: Concentration and phosphorylation levels of the SR protein SRSF1 in endometrium and dermis fibroblasts. Cell extracts were prepared from matching sets of primary endometrial (E) and dermal (D) fibroblasts and analyzed by Western blotting. (A) Proteins were probed with antibodies recognizing phosphorylated SR proteins (mAb104), glyceraldehyde-3-phosphate dehydrogenase as well as ERK in both its phosphorylated and unmodified states. (B) The relative amount of SRSF1 protein was quantified with the Odyssey Infrared Imaging system, using actin levels to normalize. Data points from five independent experiments performed with endometrium (●) and dermis (○) are plotted, and the median value is indicated. The two-tailed *p* value was determined with the Mann–Whitney rank sum test. ***p = 0.0003. (C) The phosphorylation pattern of SRSF1 in endometrium and dermis fibroblasts was determined by 2D gel electrophoresis. The pH range and the molecular weight markers (in kilodaltons) are indicated.

fibrillar adhesions also play an important role (Mao and Schwarzbauer, 2005; Frantz *et al.*, 2010). Given that endometrium and dermis fibroblasts display distinct labeling patterns for both vinculin and integrin αV, an integrin also involved in FN fibril assembly (Leiss *et al.*, 2008), these interactions could differ in these two types of fibroblasts and also contribute to differences in their respective FN fibril meshworks.

We found that expression levels of most of the tested adhesion proteins and ECM components were similar in dermis and endometrium fibroblasts, with the notable exceptions of fibronectin and collagen IV. Previous studies on fibroblasts from distinct anatomical sites underlined the existence of site-specific gene expression programs (Chang *et al.*, 2002; Rinn *et al.*, 2006). We found, as they did, that tissue-dependant differences surpassed donor-to-donor differences. In addition, the expression of the EDA+ FN splicing isoform in endometrium, a tissue that undergoes cyclical regeneration, is consistent with the documented expression of EDA+ FN in adult tissues in response to injury (Ffrench-Constant *et al.*, 1989; Muro *et al.*, 2003). Of interest, the alternatively spliced EDA domain is also highly expressed in the neovasculature of metastases, underlying its role in host tissue invasion (Rybak *et al.*, 2007).

Our data emphasize the possible discrepancies between gene expression levels and their biological effects due to the occurrence of alternative splicing, a mechanism likely to relate to >90% of the human genes (Johnson *et al.*, 2003; Wang *et al.*, 2008; Barash *et al.*, 2010). Alternative mRNA splicing depends on complex mechanisms that involve not only spliceosome assembly, but also regulation by SR proteins, coupling between transcription and splicing machineries, and epigenetic regulation (Kadener *et al.*, 2001; Nogues *et al.*, 2002; Chen and Manley, 2009; Hartmann and Valcarcel, 2009; Luco *et al.*, 2010, 2011; Munoz *et al.*, 2010). Inclusion of the EDA domain in human fibronectin is facilitated by the SR protein SRSF1, as previously demonstrated (Cramer *et al.*, 1999; Buratti and Baralle, 2004; Chen and Manley, 2009; de la Mata *et al.*, 2010) and confirmed here in endometrium fibroblasts. We found twofold higher expression levels of SRSF1 in endometrium than in dermis, a modest difference nonetheless sufficient to provide a transformed phenotype to immortal murine fibroblasts (Karni *et al.*, 2007). Because SRSF1 activity also depends on its phosphorylation pattern and AKT-dependent SRSF1 phosphorylation results in increased EDA exon inclusion (Blaustein *et al.*, 2005), we checked SRSF1 phosphorylation rates in dermis and endometrium fibroblasts and found no difference. Reports suggest that SRSF1 can be regulated by other posttranslational modifications, such as arginine methylation (Sinha *et al.*, 2010), or posttranscriptional processes, such as nonsense-mediated mRNA decay (Sun *et al.*, 2010; Valacca *et al.*, 2010). Determining whether such mechanisms can further differentiate SRSF1 activity in dermis and endometrium fibroblasts requires further investigation.

Other SR proteins, such as SRSF7 (9G8) (Cramer *et al.*, 1999) and SRSF5 (SRp40; Kuo *et al.*, 2002), as well as splicing factors, notably SPF45 (Al-Ayoubi *et al.*, 2012), can favor EDA exon inclusion in some tissues, as seen for SRSF5 in chondrocytes but not HeLa cells. Our comparison of SR protein expression/phosphorylation patterns in dermis and endometrium, using the mAb104 antibody, showed significant differences between dermis and endometrium fibroblasts, which presumably relate to other SR proteins than SRSF1. Because small interfering RNA (siRNA) depletion of SRSF1 in endometrium led to a twofold decrease of the EDA PSI value, reaching levels close to that of dermis, however, SRSF1 most likely plays a major role for EDA exon inclusion in these cells.

In conclusion, the differential fibronectin splicing between dermis and endometrium described here and the resulting differential
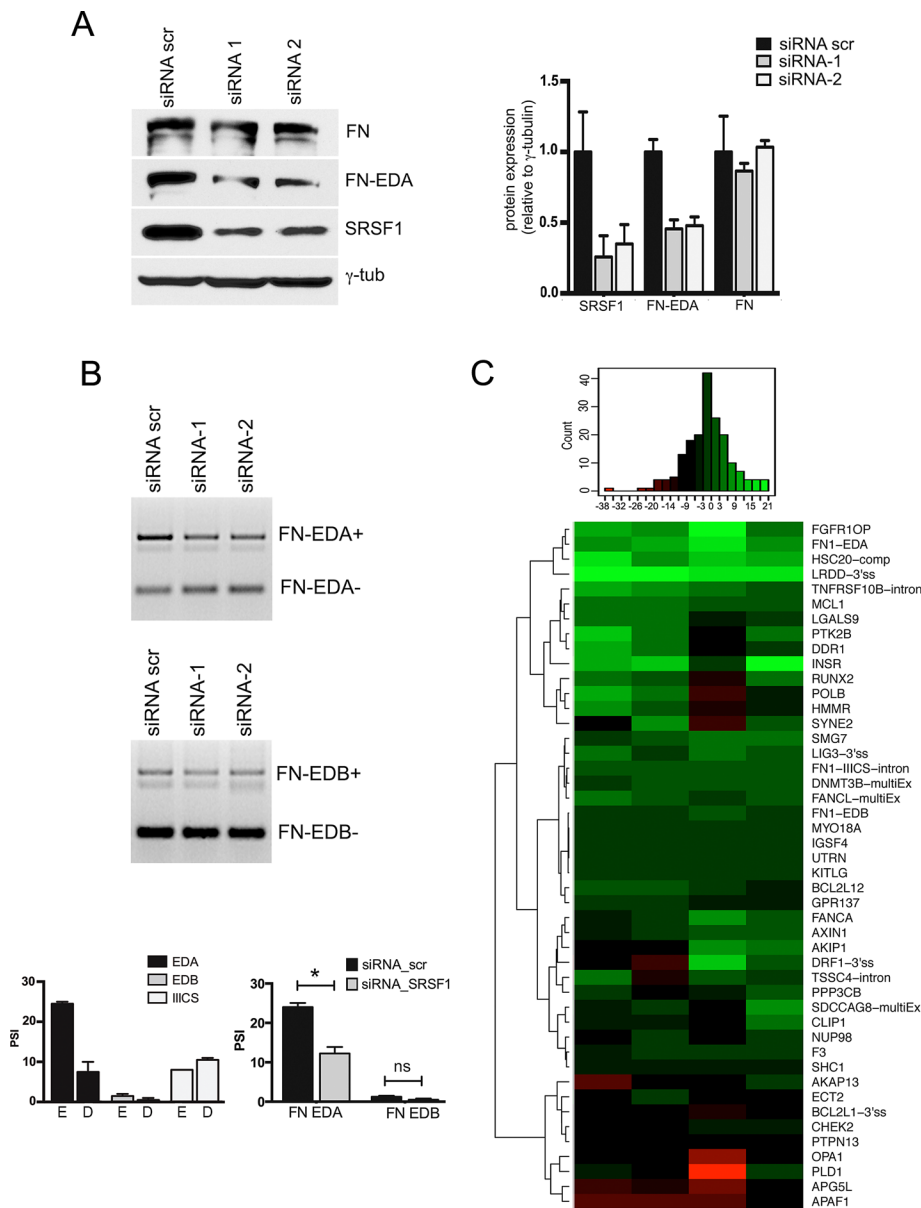
FIGURE 9: Silencing of SRSF1 in endometrium reduces inclusion of fibronectin EDA exon. (A) For silencing experiments, transfections were performed with two SRSF1-targeting siRNAs (siRNA1 and siRNA2), as well as with a scrambled siRNA (siRNA scr), which was used as a control. Data obtained with cells recovered 3 d after the siRNA transfection (similar data were obtained with two rounds of 3-d transfections, with cells collected at day 6). Total protein extracts were analyzed by Western blotting for total FN, FN containing the EDA domain, SRSF1, and, as a loading control, γ-tubulin. Relative protein values were normalized to γ-tubulin concentrations. (B) Fibronectin alternative splicing in each condition was tested by RT-PCR, using primers encompassing the alternatively spliced EDA and EDB domains. PCR products were analyzed by gel electrophoresis. (A, B) Mean values with SEM. The p values were determined by a paired t test: for FN EDA, p = 0.013 (*); for FN EDB, p = 0.058 (ns). (C) In addition, control and siRNA-treated RNA samples (n = 4 per group) were compared at the Sherbrooke RNomics platform to determine PSI for 46 alternative splicing events, including the EDA and EDB exon alternative splicings. The results are presented as a heat map showing the unsupervised hierarchical clustering of the change in splicing (ΔPSI = PSI value of the control endometrium − PSI value of the SRSF1-depleted endometrium). Splicing changes (ΔPSI values) are represented in shades of bright green (exon skipping upon SRSF1 depletion) to red (exon inclusion), as schematized in the color key histogram.

ECM capacity to support trophoblast migration provide an example of how components of the stroma can undergo different alternative splicing regulation and consequently demonstrate distinct permis-siveness to epithelial cell invasion. Alternative splicing is regulated according to cell type. We show here that, even for the same cell type, alternative splicing can differ and depend on the tissue of origin of these cells. We propose that the mechanisms brought to light here for EVCT invasion might apply as well to other types of epithelial cell invasion, thus opening new avenues for understanding the complex role played by the stroma in tissue invasion. In the case of pathological processes such as cancer progression, such mechanisms might contribute to the selected tropism of metastases (Barkan et al., 2010). It also will be worth asking whether the known interactions between cancer and stromal cells might modify SRSF1 expression rate in the latter and further promote cancer cell invasion.

MATERIALS AND METHODS

Patients and samples

Endometrial and subpubic dermal tissues were obtained from pregnant women (n = 4) undergoing C-sections at the Hospital Arnaud de Villeneuve, Montpellier, France. They were at term for a normal pregnancy. Trophoblast villi were isolated from placentas (n = 14) obtained from legal early pregnancy terminations of uncomplicated, unwanted pregnancies. Abortions were induced by mifepristone. All samples were obtained at 4- to 7-wk gestational age. Pregnancy was dated by echography and measurement of both the crown–rump length and mean gestational sac diameter. All samples were obtained after informed written consent of the patients, and the protocol was approved by the local ethics committee. For the isolation of human fibroblasts, 2-mm-long endometrium and dermis explants were mechanically chopped and seeded on 6-cm dishes in DMEM supplemented with 10% heat-inactivated fetal bovine serum (FBS). These fibroblasts were passaged twice a week and used before passage 6. All human primary cell lines of dermis and endometrium fibroblasts were checked to be mycoplasma free. They were positive for vimentin expression.

Establishment of cocultures

Cocultures were established as described previously (Fafet et al., 2008). Briefly, after uterine evacuation, placentas were immediately collected in "DMEM medium": DMEM supplemented with heat-inactivated FBS 10%, fluconazole (4 µg/ml; Pfizer, New York, NY), and amphotericin B (20 µg/ml; Bristol-Myers Squibb, New York, NY). Before dissection, placentas were gently washed with warm phosphate-buffered saline (PBS) to eliminate blood. Placental villosities were dissected with sterile tweezers
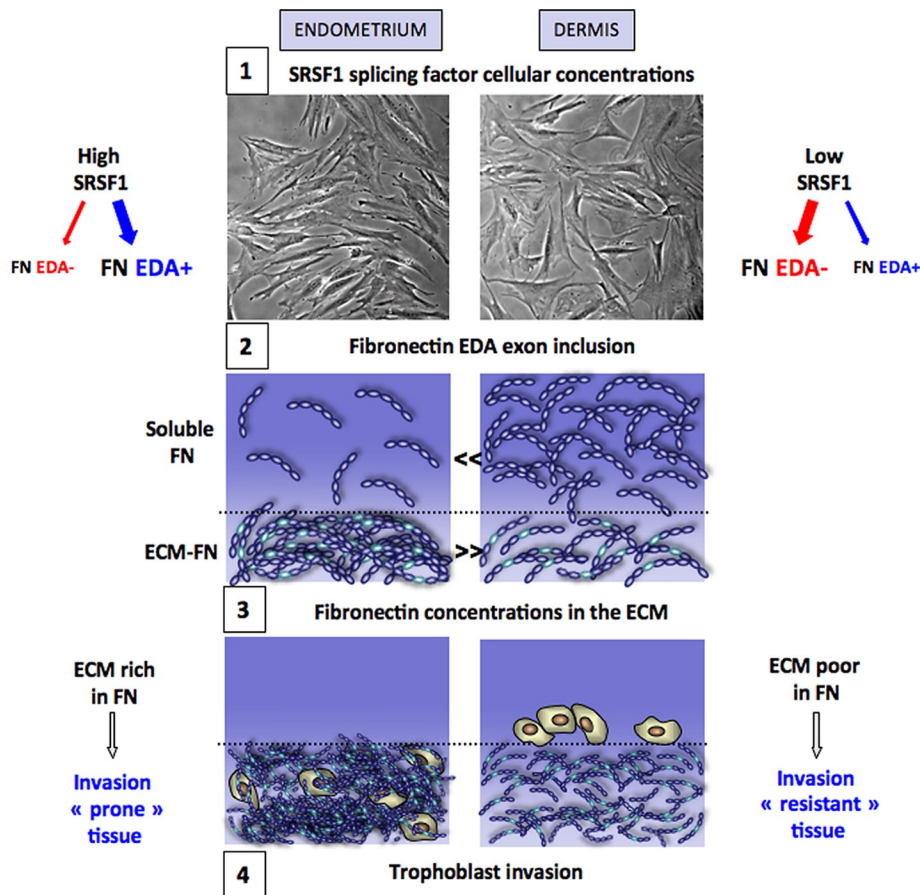
FIGURE 10: Mechanisms for the different capacities of endometrium and dermis tissues to support trophoblast invasion. 1) Endometrium fibroblasts produce higher concentrations of the SR protein SRSF1 than dermis fibroblasts, which leads 2) to higher inclusion rates of the EDA exon in the fibronectin produced by endometrium and consequently 3) to an endometrium extracellular matrix that contains more and thicker fibronectin bundles than dermis. 4) This results in a better capacity for the endometrium tissue than for dermis to support trophoblast invasion.

and scissors to get tissue pieces ~1 mm long. Villosities were then rinsed once and resuspended in DMEM/Ham medium: 50% of DMEM and 50% of Ham F12 medium supplemented with $CaCl_2$ (2 mM), $MgSO_4$ (2 mM), and $NaHCO_3$ (0.5 mM). Three days before the coculture, the endometrial and dermal fibroblasts were seeded on glass coverslips (10^5 cells in 35-mm-diameter dishes) in DMEM supplemented with FBS 10% so that fibroblasts were confluent by the time cocultures were started. Before setting up the cocultures, the fibroblast medium was changed to DMEM/Ham medium. Approximately 10 trophoblast explants were seeded per 35-mm dish and let to adhere for 16 h at 37°C. At that point, the medium was aspirated, and plates were rinsed once with the DMEM/Ham medium to eliminate all unattached villosities and further incubated in the same medium. This was considered to be time zero for all analyses of trophoblast migration. When appropriate, the supplementation of dermal fibroblasts with fibronectin (human plasma FN; BD Biosciences, San Jose, CA) was done at the time of fibroblast seeding with the addition of 50 μg of fibronectin/35-mm dish.

In vitro 3D cultures

The 3D cultures were set in 48-well plates. Collagen I was used at a final concentration of 1.5 mg/ml. When indicated, fibronectin (human plasma FN; BD Biosciences) was mixed with collagen at a final concentration of 5 μg/ml. A first layer of collagen matrix was deposited in the wells and incubated at 37°C. Placental 1-mm-long explants were then deposited on the matrix, and a second layer of collagen matrix was poured on top of the explants. The wells were then filled with DMEM supplemented with FBS 5% and incubated at 37°C.

siRNA transfection

siRNAs directed against SRSF1 were transfected at a concentration of 100 nM with Oligofectamine reagent (Invitrogen, Carlsbad, CA) according to the manufacturer's instructions. Briefly, the day before transfection endometrial fibroblasts (10^5 cells) were seeded in 35-mm dishes in DMEM supplemented with FBS 10%. Fibroblasts were ~40% confluent the day of transfection. Cell culture media was replaced by 800 μl of serum-free Opti-MEM medium (Invitrogen) before transfection. A mixture of 10 μl of siRNAs (10 μM) diluted in 175 μl of Opti-MEM and 4 μl of Oligofectamine diluted in 7.5 μl of Opti-MEM was incubated for 10 min at room temperature, then mixed gently and further incubated for another 15 min before addition dropwise to the cells. The cells were incubated 4 h at 37°C before addition of DMEM supplemented with FBS 10%. Cells were recovered 72 h after transfection for RNA or protein extraction (day 3 experiments) or reseeded to undergo a second round of transfection (day 6 experiments). Sequences used are the following: siRNA scrambled, 5'-GUG-AAG-CGC-AAG-UAG-ACU-AdTdT-3' and 5'-UAG-UCU-ACU-UGC-GCU-UCA-CdTdT-3'; siRNA 1, 5'-GGG-UAG-CAA-UGC-CAG-UAA-AdTdT-3' and 5'-UUU-ACU-GGC-AUU-GCU-ACC-CdTdT-3'; siRNA 2, 5'-GAA-AGA-AGA-UAU-GAC-CUA-UdTdT-3' and 5'-AUA-GGU-CAU-AUC-UUC-UUU-CdTdT-3'.

Determination of the percent splicing index

The RNA samples were analyzed by the RNomics platform of Sherbrooke University (http://lgfus.ca/public/fr/node/22). A total of 46 alternative splicing units were tested by endpoint PCR. Microcapillary electrophoresis (using the LabChip HT DNA assay on a Caliper [Hopkinton, MA] automated microfluidic station) was used for the detection and characterization of alternative splicing events. The relative concentrations of alternatively spliced mRNA isoforms were determined, and the PSI was calculated. For bioinformatic analysis, Ward hierarchical clustering using an Euclidean distance metric was done using R-based open-access software (www.r-project.org/; www.hiv.lanl.gov/content/sequence/HEATMAP/heatmap.html).

Imaging

Time-lapse analysis of trophoblastic cell invasion was done with a phase-contrast Leica DMIR (Leica, Wetzlar, Germany) in an incubation chamber providing controlled temperature, CO_2 concentration, and hygrometry. Pictures were taken every 8 min for 24-48 h using an ORCA 100 (Hamamatsu, Hamamatsu, Japan) and the HPDCPx32

program. After imaging, all time points were compiled and exported as a QuickTime (Apple, Cupertino, CA; avi) file using MetaMorph software (Molecular Devices, Sunnyvale, CA). Alternatively, images were taken with a DMIRE 2 2002 microscope (Leica) and a MicroMax 1300Y/HS (19xx) camera (Roper Scientific, Trenton, NJ) with the Meta-Morph 7 acquisition program. For phase-contrast microscopy of both cocultures and 3D cultures, photographs were taken on an Axiovert 25 inverted-phase microscope (Carl Zeiss, Jena, Germany) coupled to a digital PowerShot camera (Canon, Melville, NY). The digitalized images were mounted using Photoshop (Adobe, San Jose, CA). Immunofluorescence and CellTracker stainings were visualized with a Zeiss LSM 510 Meta confocal laser system. Images were converted with MetaMorph and processed with Photoshop software.

Data statistical analysis

Sample comparison was performed using the Mann–Whitney rank sum test. Statistical analysis and data plots were performed using Prism software (GraphPad, San Diego, CA). $*p \leq 0.05$; $**p \leq 0.01$; $***p \leq 0.001$.

Miscellaneous

A detailed description of cytoimmunofluorescence, protein analysis, and RNA quantification (RT-qPCR) conditions is given in the Supplemental Experimental Procedures.

REFERENCES

Abe Y, Bui-Thanh NA, Ballantyne CM, Burns AR (2005). Extra domain A and type III connecting segment of fibronectin in assembly and cleavage. Biochem Biophys Res Commun 338, 1640–1647.

Al-Ayoubi AM, Zheng H, Liu Y, Bai T, Eblen ST (2012). Mitogen-activated protein kinase phosphorylation of splicing factor 45 (SPF45) regulates SPF45 alternative splicing site utilization, proliferation, and cell adhesion. Mol Cell Biol 32, 2880–2893.

Aplin JD, Haigh T, Jones CJ, Church HJ, Vicovac L (1999). Development of cytotrophoblast columns from explanted first-trimester human placental villi: role of fibronectin and integrin alpha5beta1. Biol Reprod 60, 828–838.

Astrof S, Crowley D, Hynes RO (2007). Multiple cardiovascular defects caused by the absence of alternatively spliced segments of fibronectin. Dev Biol 311, 11–24.

Barash Y, Calarco JA, Gao W, Pan Q, Wang X, Shai O, Blencowe BJ, Frey BJ (2010). Deciphering the splicing code. Nature 465, 53–59.

Barkan D, Green JE, Chambers AF (2010). Extracellular matrix: a gatekeeper in the transition from dormancy to metastatic growth. Eur J Cancer 46, 1181–1188.

Bischof P, Haenggeli L, Campana A (1995). Gelatinase and oncofetal fibronectin secretion is dependent on integrin expression on human cytotrophoblasts. Hum Reprod 10, 734–742.

Blaustein M et al. (2005). Concerted regulation of nuclear and cytoplasmic activities of SR proteins by AKT. Nat Struct Mol Biol 12, 1037–1044.

Blaustein M, Quadrana L, Risso G, Mata Mde L, Pelisch F, Srebrow A (2009). SF2/ASF regulates proteomic diversity by affecting the balance between translation initiation mechanisms. J Cell Biochem 107, 826–833.

Buratti E, Baralle FE (2004). Influence of RNA secondary structure on the pre-mRNA splicing process. Mol Cell Biol 24, 10505–10514.

Chang HY, Chi JT, Dudoit S, Bondre C, van de Rijn M, Botstein D, Brown PO (2002). Diversity, topographic differentiation, and positional memory in human fibroblasts. Proc Natl Acad Sci USA 99, 12877–12882.

Chen M, Manley JL (2009). Mechanisms of alternative splicing regulation: insights from molecular and genomics approaches. Nat Rev Mol Cell Biol 10, 741–754.

Cramer P, Caceres JF, Cazalla D, Kadener S, Muro AF, Baralle FE, Kornblihtt AR (1999). Coupling of transcription with alternative splicing: RNA pol II promoters modulate SF2/ASF and 9G8 effects on an exonic splicing enhancer. Mol Cell 4, 251–258.

Cramer P, Pesce CG, Baralle FE, Kornblihtt AR (1997). Functional association between promoter structure and transcript alternative splicing. Proc Natl Acad Sci USA 94, 11456–11460.

Damsky CH, Librach C, Lim KH, Fitzgerald ML, McMaster MT, Janatpour M, Zhou Y, Logan SK, Fisher SJ (1994). Integrin switching regulates normal trophoblast invasion. Development 120, 3657–3666.

de la Mata M, Alonso CR, Kadener S, Fededa JP, Blaustein M, Pelisch F, Cramer P, Bentley D, Kornblihtt AR (2003). A slow RNA polymerase II affects alternative splicing in vivo. Mol Cell 12, 525–532.

de la Mata M, Lafaille C, Kornblihtt AR (2010). First come, first served revisited: factors affecting the same alternative splicing event have different effects on the relative rates of intron removal. RNA 16, 904–912.

Fafet P, Rebouissou C, Maudelonde T, Vignais ML (2008). Opposite effects of transforming growth factor-beta activation and rho-associated kinase inhibition on human trophoblast migration in a reconstituted placental-endometrial coculture system. Endocrinology 149, 4475–4485.

Feinberg RF, Kliman HJ, Lockwood CJ (1991). Is oncofetal fibronectin a trophoblast glue for human implantation? Am J Pathol 138, 537–543.

Ffrench-Constant C, Van de Water L, Dvorak HF, Hynes RO (1989). Reappearance of an embryonic pattern of fibronectin splicing during wound healing in the adult rat. J Cell Biol 109, 903–914.

Frantz C, Stewart KM, Weaver VM (2010). The extracellular matrix at a glance. J Cell Sci 123, 4195–4200.

Friedl P, Alexander S (2011). Cancer invasion and the microenvironment: plasticity and reciprocity. Cell 147, 992–1009.

George EL, Georges-Labouesse EN, Patel-King RS, Rayburn H, Hynes RO (1993). Defects in mesoderm, neural tube and vascular development in mouse embryos lacking fibronectin. Development 119, 1079–1091.

Guan JL, Trevithick JE, Hynes RO (1990). Retroviral expression of alternatively spliced forms of rat fibronectin. J Cell Biol 110, 833–847.

Harris LK, Jones CJ, Aplin JD (2009). Adhesion molecules in human trophoblast—a review. [II] Extravillous trophoblast. Placenta 30, 299–304.

Hartmann B, Valcarcel J (2009). Decrypting the genome's alternative messages. Curr Opin Cell Biol 21, 377–386.

Heino J (2007). The collagen family members as cell adhesion proteins. Bioessays 29, 1001–1010.

Johnson JM, Castle J, Garrett-Engele P, Kan Z, Loerch PM, Armour CD, Santos R, Schadt EE, Stoughton R, Shoemaker DD (2003). Genome-wide survey of human alternative pre-mRNA splicing with exon junction microarrays. Science 302, 2141–2144.

Joyce JA, Pollard JW (2009). Microenvironmental regulation of metastasis. Nat Rev Cancer 9, 239–252.

Kadener S, Cramer P, Nogues G, Cazalla D, de la Mata M, Fededa JP, Werbajh SE, Srebrow A, Kornblihtt AR (2001). Antagonistic effects of T-Ag and VP16 reveal a role for RNA pol II elongation on alternative splicing. EMBO J 20, 5759–5768.

Kadener S, Fededa JP, Rosbash M, Kornblihtt AR (2002). Regulation of alternative splicing by a transcriptional enhancer through RNA pol II elongation. Proc Natl Acad Sci USA 99, 8185–8190.

Kadler KE, Hill A, Canty-Laird EG (2008). Collagen fibrillogenesis: fibronectin, integrins, and minor collagens as organizers and nucleators. Curr Opin Cell Biol 20, 495–501.

Karni R, de Stanchina E, Lowe SW, Sinha R, Mu D, Krainer AR (2007). The gene encoding the splicing factor SF2/ASF is a proto-oncogene. Nat Struct Mol Biol 14, 185–193.

Kuo BA, Uporova TM, Liang H, Bennett VD, Tuan RS, Norton PA (2002). Alternative splicing during chondrogenesis: modulation of fibronectin exon EIIIA splicing by SR proteins. J Cell Biochem 86, 45–55.

Leiss M, Beckmann K, Giros A, Costell M, Fassler R (2008). The role of integrin binding sites in fibronectin matrix assembly in vivo. Curr Opin Cell Biol 20, 502–507.

Luco RF, Allo M, Schor IE, Kornblihtt AR, Misteli T (2011). Epigenetics in alternative pre-mRNA splicing. Cell 144, 16–26.

Luco RF, Pan Q, Tominaga K, Blencowe BJ, Pereira-Smith OM, Misteli T (2010). Regulation of alternative splicing by histone modifications. Science 327, 996–1000.

Lu P, Weaver VM, Werb Z (2012). The extracellular matrix: a dynamic niche in cancer progression. J Cell Biol 196, 395–406.

Manabe R, Ohe N, Maeda T, Fukuda T, Sekiguchi K (1997). Modulation of cell-adhesive activity of fibronectin by the alternatively spliced EDA segment. J Cell Biol 139, 295–307.

Mao Y, Schwarzbauer JE (2005). Fibronectin fibrillogenesis, a cell-mediated matrix assembly process. Matrix Biol 24, 389–399.

McKeown-Longo PJ, Etzler CA (1987). Induction of fibronectin matrix assembly in human fibrosarcoma cells by dexamethasone. J Cell Biol 104, 601–610.

Mermoud JE, Cohen PT, Lamond AI (1994). Regulation of mammalian spliceosome assembly by a protein phosphorylation mechanism. EMBO J 13, 5679–5688.

Misteli T, Caceres JF, Clement JQ, Krainer AR, Wilkinson MF, Spector DL (1998). Serine phosphorylation of SR proteins is required for their recruitment to sites of transcription in vivo. J Cell Biol 143, 297–307.

Misteli T, Caceres JF, Spector DL (1997). The dynamics of a pre-mRNA splicing factor in living cells. Nature 387, 523–527.

Moretti FA, Chauhan AK, Iaconcig A, Porro F, Baralle FE, Muro AF (2007). A major fraction of fibronectin present in the extracellular matrix of tissues is plasma-derived. J Biol Chem 282, 28057–28062.

Munoz MJ, de la Mata M, Kornblihtt AR (2010). The carboxy terminal domain of RNA polymerase II and alternative splicing. Trends Biochem Sci 35, 497–504.

Muro AF, Chauhan AK, Gajovic S, Iaconcig A, Porro F, Stanta G, Baralle FE (2003). Regulated splicing of the fibronectin EDA exon is essential for proper skin wound healing and normal lifespan. J Cell Biol 162, 149–160.

Nguyen DX, Bos PD, Massague J (2009). Metastasis: from dissemination to organ-specific colonization. Nat Rev Cancer 9, 274–284.

Nogues G, Kadener S, Cramer P, Bentley D, Kornblihtt AR (2002). Transcriptional activators differ in their abilities to control alternative splicing. J Biol Chem 277, 43110–43114.

Nogués G, Muñoz MJ, Kornblihtt AR (2003). Influence of polymerase II processivity on alternative splicing depends on splice site strength. J Biol Chem 278, 52166–52171.

Norwitz ER, Schust DJ, Fisher SJ (2001). Implantation and the survival of early pregnancy. N Engl J Med 345, 1400–1408.

Paget S (1889). The distribution of secondary growths in cancer of the breast. Lancet 1, 571–573.

Pankov R, Yamada KM (2004). Non-radioactive quantification of fibronectin matrix assembly. Curr Protoc Cell Biol, Chapter 10, Unit 10.13.

Peters DM, Portz LM, Fullenwider J, Mosher DF (1990). Co-assembly of plasma and cellular fibronectins into fibrils in human fibroblast cultures. J Cell Biol 111, 249–256.

Rinn JL, Bondre C, Gladstone HB, Brown PO, Chang HY (2006). Anatomic demarcation by positional variation in fibroblast gene expression programs. PLoS Genet 2, e119.

Rybak JN, Roesli C, Kaspar M, Villa A, Neri D (2007). The extra-domain A of fibronectin is a vascular marker of solid tumors and metastases. Cancer Res 67, 10948–10957.

Sen S, Talukdar I, Webster NJ (2009). SRp20 and CUG-BP1 modulate insulin receptor exon 11 alternative splicing. Mol Cell Biol 29, 871–880.

Singh P, Carraher C, Schwarzbauer JE (2010). Assembly of fibronectin extracellular matrix. Annu Rev Cell Dev Biol 26, 397–419.

Sinha R, Allemand E, Zhang Z, Karni R, Myers MP, Krainer AR (2010). Arginine methylation controls the subcellular localization and functions of the oncoprotein splicing factor SF2/ASF. Mol Cell Biol 30, 2762–2774.

Sottile J, Shi F, Rublyevska I, Chiang HY, Lust J, Chandler J (2007). Fibronectin-dependent collagen I deposition modulates the cell response to fibronectin. Am J Physiol Cell Physiol 293, C1934–C1946.

Soundararajan R, Rao AJ (2004). Trophoblast "pseudo-tumorigenesis": significance and contributory factors. Reprod Biol Endocrinol 2, 15.

Sun S, Zhang Z, Sinha R, Karni R, Krainer AR (2010). SF2/ASF autoregulation involves multiple layers of post-transcriptional and translational control. Nat Struct Mol Biol 17, 306–312.

Valacca C, Bonomi S, Buratti E, Pedrotti S, Baralle FE, Sette C, Ghigna C, Biamonti G (2010). Sam68 regulates EMT through alternative splicing-activated nonsense-mediated mRNA decay of the SF2/ASF proto-oncogene. J Cell Biol 191, 87–99.

Venables JP et al. (2013). RBFOX2 is an important regulator of mesenchymal-specific splicing in both normal and cancer tissues. Mol Cell Biol 33, 396–405.

Wang ET, Sandberg R, Luo S, Khrebtukova I, Zhang L, Mayr C, Kingsmore SF, Schroth GP, Burge CB (2008). Alternative isoform regulation in human tissue transcriptomes. Nature 456, 470–476.

White ES, Baralle FE, Muro AF (2008). New insights into form and function of fibronectin splice variants. J Pathol 216, 1–14.

White ES et al. (2010). Control of fibroblast fibronectin expression and alternative splicing via the PI3K/Akt/mTOR pathway. Exp Cell Res 316, 2644–2653.

Zahler AM, Neugebauer KM, Stolk JA, Roth MB (1993). Human SR proteins and isolation of a cDNA encoding SRp75. Mol Cell Biol 13, 4023–4028.

Zoppi N, Ritelli M, Colombi M (2012). Type III and V collagens modulate the expression and assembly of EDA(+) fibronectin in the extracellular matrix of defective Ehlers-Danlos syndrome fibroblasts. Biochim Biophys Acta 1820, 1576–1587.